International Journal of Oceans and Oceanography
ISSN 0973-2667 Volume 11, Number 1 (2017), pp. 105-119

http://www.ripublication.com

Oceanic Image Dehazing based on Red Color Priority using Segmentation Approach

S. B. Borkar*
Research Scholar, Department of Electronics and Telecommunication,
SGGS Institute of Engineering and Technology, Nanded-431606, Maharashtra, India.

S. V. Bonde
Professor, Department of Electronics and Telecommunication,
SGGS Institute of Engineering and Technology, Nanded-431606, Maharashtra, India.

Abstract

Images captured underwater faces inherent problem of haze on account of marine snow and small floating particles. Moreover, these underwater oceanic images are characterized by non-homogeneous haze. Over the time, a number of classical enhancement techniques like histogram equalization, homomorphic filtering, Retinex method have been successfully implemented for image restoration. However, these approaches do not provide satisfactory outcomes like optimum visibility recovery, color fidelity, and improved contrast for underwater images. In this study, we propose an algorithm in which underwater images are segmented based on non-homogeneous haze and then dehazing is carried out using the single red color channel in RGB space as it attenuates maximum in the underwater scenario. The proposed approach has three main steps to address above problems. First, a segmentation of image is proposed to separate foreground and background of the image using k-means clustering algorithm. Secondly, a depth map is derived based on red color priority using effective morphological operation. Finally, the post-processing has been performed by obtaining enhanced image using contrast stretching operation. The main advantage offered by the proposed algorithm is that it can be very effective in detecting hazy regions and exhibit overall natural preservation in color fidelity along the relative haze depths.

Keywords: Underwater Image Analysis, Image segmentation, k-means Clustering, Image Restoration.

* *Corresponding Author E-mail:borkarsamarth@sggs.ac.in*

I. INTRODUCTION

A great deal of research has been undergoing towards the exploration of ocean bed for archaeological surveying, laying of communication links, and study of flora and fauna to understand the effect of a change in climatic conditions on oceanic biodiversity due to artificial activities. This necessitates the capturing of underwater images for decision making. The images procured underwater are hazy in an appearance on account of small floating particles and marine snow contributing to turbidity. To overcome the limited visibility in turbid underwater regions, an artificial source of lighting is employed. The natural process of attenuation and scattering of light result in degradation of color, lowering of contrast and effect of blurring [1]. The propagation of color depth in underwater is a direct function of the corresponding wavelength of color. Red color has the longest wavelength and lesser energy as compared to the green and blue counterpart, and as a consequence red color travels the shortest distance and blue and green color casts dominance in the image appearance. Applying such images for decision-making algorithms in computer vision applications like automatic underwater vehicles and other underwater robotic mission demands to pre-process hazy images.

The approaches to addressing these image restoration problems are diversely grouped based on the single input image or multiple input images of the same scene captured from distinctive positions and at different time intervals, and polarization [2] and [3]. Theoretically, this technique sounds excellent but practically to generate a database for an underwater application involves computationally high-end resources such as laser lighting and polarized cameras. So researchers opted for an alternative like single image based restoration methods, where there is no reference image to bank upon and the user has to recover the enhanced image by processing the given single hazy image.

The technique which has gained wide popularity amongst researchers to estimate the haze depth is proposed in [4]. In this article, the author calculates the depth map and extent of transmission, based on minimum pixel intensity at block level for three color planes. This study based on statistical analysis paved the way for finding the depth of haze. The major limitation of this dark channel prior (DCP) method is, for images involving sky regions and objects in the image similar to atmospheric light, the performance is not satisfactory. This method was modified for underwater application in [5]. The depth is a function of scattering parameter. The authors used predefined scattering values to solve the problem of haze. The major limitation of this approach was a selection of parameters, which changes for the same location at a different season and different time zone. The salinity of water and its associated properties also makes this assumption a vague entity.

There are many other works found in literature which primarily directed their work towards underwater image restoration based on dark channel theory, and most of them

investigated to reduce the computational exhaustiveness encountered in the state of the art technique.

In [4], researchers proposed a computationally exhaustive method to refine the transmission map. To solve this problem, researchers proposed guided filtering [6], guided trigonometric bilateral filtering [7], joint trilateral filtering [8] etc. In [9], authors proposed adaptive cross image filters and in [10] authors estimated transmission depth map using the difference in attenuation between the three color channels and proposed guided trigonometric filter. Basically, all these filters are edge preserving smoothing operators. Many authors have proposed alterations to dark channel and applied it to underwater imagery. The earliest approach proposed is based on attenuation difference amongst three color channels in an underwater scenario [11]. A variant of the dark channel, presented in [12] restores the underwater image contrast utilizing color channel with a shorter wavelength. In [13], color attenuation prior for image dehazing and contrast restoration has been proposed. In our comparative studies, we have compared our work with this innovative approach.

In this proposed work, the phenomenon of higher attenuation of the red color channel is exploited to find the depth of haze. Secondly, for underwater images, the details are much more prominent as compared to outdoor scenes and also the depth of vision is also limited. Instead of using the patch-based dehazing technique we opted for pixel level dehazing to minimize the blocking artifacts and to retain sharp details near transmission discontinuities. As discussed, the haze phenomenon thus observed in the underwater scenario is different to that observed in outdoor scenes. So, instead of opting global value of atmospheric light for the entire image, we experimented with segmenting the image into two regions based on intensity which corresponds to the difference in haze homogeneity also and referred to it as foreground and background image. The result exhibits naturalness in the image with appreciable depth factor. Finally, the post-processing is carried out using image normalization.

The paper is arranged as follows. Section I introduces the problem statement and also highlight the background and related work. Section II briefly explains the image formation model. In Section III we present our implementation of oceanic image dehazing. In Section IV, we compare our results with existing work and finally, Section V concludes our paper with future work.

II. IMAGE FORMATION MODEL

The simplified image formation model used in [14], and further developed for haze image formation model in [15] and [16] is expressed as:

$$I(x,y) = J(x,y)t(x,y) + A\big(1 - t(x,y)\big), \tag{1}$$

where $I(x,y)$ is the 2D input image to be dehazed, $J(x,y)$ is the restored image or scene radiance, A is termed as a homogeneous background light (atmospheric light) and $t(x,y)$ is the transmission depth. The first multiplicative term $J(x,y)t(x,y)$ is referred to as direct attenuation whereas the other multiplicative term, $A(1-t(x,y)$ is referred to as airlight. The equation (1) can be directly solved for scene radiance as:

$$J(x,y) = \frac{I(x,y)-A}{t(x,y)} + A, \tag{2}$$

Using Beer-Lambert's law for optical images, the radiance of the scene decreases in an exponential factor as the propagation distance increases. The transmission function is expressed as:

$$t(x,y) = e^{-\beta d(x,y)}, \tag{3}$$

where β is the coefficient of attenuation resulting out of scattering in the surrounding atmosphere and $d(x,y)$ is the span between the camera and position of an image forming the pixel coordinate (x,y).

As we see, $d(x,y) \to \infty, t(x,y) = 0,$ and this implies $I(x,y) = A(x,y),$ (4)

$d(x,y) \to 0, t(x,y) = 1,$ and this implies $I(x,y) = J(x,y),$ (5)

The above two equations underline the importance of atmospheric light value A. In natural images, the depth ranges up to the horizon and extends towards the sky at an infinite distance. In normal practice, this corresponds to most haze opaque pixel in the dark map, which is then spatially mapped to the input image to obtain the corresponding value of A. Any bright object can be misjudged as A. So to avoid this, various techniques are offered in the literature. Improper selection of A value restores the image badly.

III. PROPOSED DEHAZING ALGORITHM

As discussed above, on account of higher attenuation rate, the histogram of red color channel shifts towards darker scale for underwater images as depicted in Figure 1. Table 1 shows the mean values of individual color channel intensities.

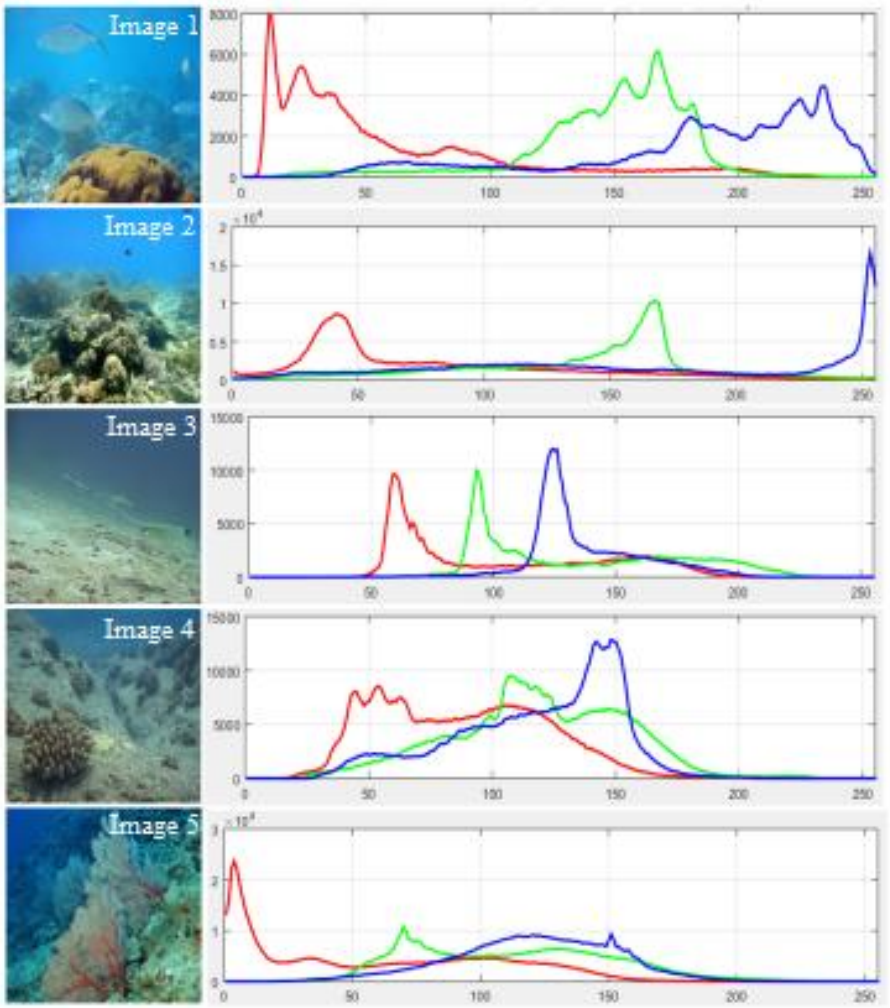

Figure 1 Histograms of Hazy underwater images used in this studies.

Table 1 RGB mean intensities of images in figure 1

Channel	Image 1	Image 2	Image 3	Image 4	Image 5
Red	55.27	77.41	101.50	86.94	57.90
Green	147.68	139.50	134.47	117.38	111.22
Blue	183.33	157.44	135.56	117.91	119.82

In the case of natural images, the background tends towards the brighter end, and typically the value of atmospheric light belongs to this background region. For underwater scenario, the background of an image tends to be on a darker side as compared to the foreground object, and as a result, the most haze opaque pixel belongs to the foreground image. The value thus chosen has an undesirable effect on dehazing of the underwater images. So we used the segmentation approach to separate the image into foreground and background part and obtained the value of A separately for each part.
Following steps are implemented in the proposed dehazing algorithm.

- Step 1 Input the underwater hazy image.
- Step 2 Transform the RGB image into L*A*B color space.
- Step 3 Implement k-means clustering on *A*B color space using k=2.
- Step 4 Use the results from *k*-means to label all the pixels.
- Step 5 Based on color, segment the images. (in our case 2 images)
- Step 6 Input the segmented image, $I_n(x, y)$, where (n=1,2)
- Step 7 Decompose the above image into individual color channels.
- Step 8 Apply a morphological operation to the red channel to obtain the dark channel image.
- Step 9 Estimate the atmospheric light A for each part.
- Step 10 Generate the transmission map.
- Step 11 Refinement of transmission map.
- Step 12 Recovery of dehazed image, $J(x, y)$
- Step 13 Combine the two separately dehazed images.
- Step 14 Post-processing using image normalization.

The detailed implementation is explained in following sections.

A. Underwater Image segmentation

It is the image background part that contributes to hazing as seen in equation (1). So separating the two regions, tends to enhance the image in a better way. As we have discussed earlier, the image is subdivided into the foreground and background parts and dehazing is applied individually to each of the parts and then combined at the final stage. In this presented work, we implement segmentation of the underwater image into foreground and background component using *k*-means clustering based on intensity

profile. It is commonly used techniques for the segmentation of a data range into k groups. The k – means clustering algorithm is as follows [17] [18].

i) Initially, decide the number of cluster centers.

ii) For every single pixel, find the Euclidean distance d for the pixel $p(x, y)$ and the rest of cluster c_k using equation (6),

$$d = \left|\left|p(x,y) - c_k\right|\right|, \tag{6}$$

iii) Based on above Euclidean distance attribute the closest cluster to each pixel.

iv) After assigning the pixels, again calculate the new position of the center using the equation (7),

$$c_k = \frac{1}{k}\sum_{y \in c_k}\sum_{x \in c_k} p(x,y)\,, \tag{7}$$

v) Repeat the above steps until it converges reasonably.

The k-means algorithm works well in underwater oceanic images if the non-homogeneous haze is distinctly separable from each other. The only shortcoming of this algorithm is that it demands apriori specification about the number of clusters. The partitioning of image and dehazing process is as shown for one underwater image in Figure 2.

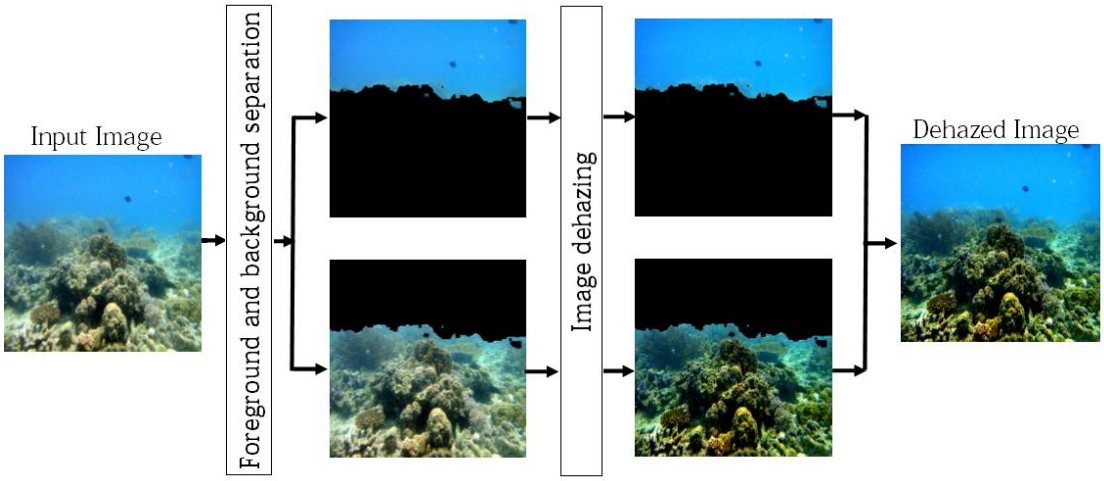

Figure 2 Segmentation of underwater image and dehazing

B. Obtaining the depth map

As far as underwater images are concerned, the visibility is limited to few meters on account of haze, turbidity and darkness nature of surrounding environment. Based on a set of images, we figured out that the pixel-wise mean intensity of red channel in underwater images are comparatively less as compared to other two channels in RGB color space, and also if we observe the histogram of three channels for underwater images, we realize that red component is shifted more towards darker shade as compared to other two channels. Whereas, similar histogram observed in natural image cases is overlapping for three color channels. So the use of all three channels to find the dark channel prior is a necessity in natural images. As seen in Figure 1 and Table 1, the red color component is predominant in the lower end of the histogram with minimal mean intensity, we can rely on this single red channel for computation of the dark map. To implement depth map, we use morphological based operation, which is computationally not exhaustive. This feature is very important when one considers a real-time application. Inspired from dark channel prior [4], we derive the modified red color priority depth map image, which is given as:

$$I_R^{dark}(x,y) = \min_{\lambda \epsilon R}\left(\min_{y \epsilon \Omega(x,y)} (I_R^n(x,y))\right), \tag{8}$$

where $\Omega(x,y)$ is the structuring element, λ corresponds to wavelength and R corresponds to the red color channel. This depth map gives the pictorial estimate of the presence of haze and is effectively useful for estimating the transmission map.

C. Computation of atmospheric light

Also termed as homogeneous light, is an important factor to obtain a dehazed image. For computing the value of this atmospheric light A, we screen the dark map image as expressed in equation (8) and find the most haze opaque pixel in it. This pixel location is then mapped spatially to RGB image and the corresponding intensity of the pixel in the normalized image is selected. This technique works satisfactorily for the underwater image. As in our case since we segment the image into foreground and background, we compute two value of A, unique to each region and proceed with dehazing.

D. Obtaining the transmission map

A transmission map gives the extent of light reaching the camera in a degraded image. The dark map derived out of red channel prior is used to obtain this transmission map. This is the most important clue as to determine the extent and depth of the hazy image and light transmission in an image formation process. The equation used for obtaining the transmission map is as follows:

$$\min_{x,y \epsilon \Omega(x,y)} \big(I_\lambda(x,y)\big) = \tilde{t}(x,y) \min_{y \epsilon \Omega(x,y)} \big(J_\lambda(x,y) + A(1 - t_\lambda(x,y)\big), \tag{9}$$

Applying minimum operation for the red color channel:

$$\min_{\lambda \epsilon R} \min_{x,y \epsilon \Omega(x,y)} (I_\lambda(x,y)/A) = \min_{\lambda \epsilon R} \{ \min_{x,y \epsilon \Omega(x,y)} \left(\frac{J_\lambda(x,y)}{A} \right) \tilde{t}(x,y) + \min_{\lambda \epsilon R} \left(1 - \tilde{t}(x,y)\right), \quad (10)$$

and rearranging the equation, we obtain the equation for transmission map. In this equation, we introduce a constant parameter *w.*

$$\tilde{t}(x,y) = 1 - w * \min_{\lambda \epsilon R} \left\{ \min_{x,y \epsilon \Omega(x,y)} \left(\frac{I_\lambda(x,y)}{A} \right) \right\}, \quad (11)$$

where the selection of parameter *w* is chosen to preserve some amount of haze so that the final image looks natural. A higher value of *w* results into the complete removal of haze making the image look unrealistic and lower value of *w* results into lower intensity image and makes it darker. The value of *w* ranges between 0 and 1 in a normalized image. In all our experiments conducted for this article, we have chosen *w* = 0.70. This value gives the best possible results for typical underwater images.

E. Refinement of transmission map

On account of the pixel based operation, the transmission map generated appears pixelated. If used as it is in the equation (1) to recover the scene radiance, the final dehazed image will thus look pixelated. This transmission map needs to be smoothened. We obtained satisfying results with a filter as proposed in [19] to smoothen the transmission map.

F. Recovery of the dehazed image

The scene radiance is then obtained using the equation (12)

$$J(x,y) = \frac{I(x,y) - A}{\max(t(x,y), to)} + A, \quad (12)$$

Now, we have underwater hazy image $I(x,y)$, the refined transmission image $t(x,y)$, and the background light A. Also, it has been observed that $t(x,y)$, can be zero for higher value of haze component. So as to avoid mathematical error in the equation (12) it is suggested to limit the transmission $t(x,y)$, to a minimum value of to.

G. Post Processing to restore the image

The images obtained using dark channel prior results in the overall darker shade so was the case with red channel prior too. To address this problem, we used a simple image normalization (contrast stretching) [20] and image adjusting operation. In our application, we have stretched the three channels using the same offset and scaling so as to retain the effective color ratios.

IV. RESULT AND ANALYSIS

The performance of the algorithm proposed in this paper is tested quantitatively as well as qualitatively. Both outcomes exhibit superior performance in the removal of haze and color restoration ability. In this study, we compare the results of our method to He *et al*.'s model (2011), Chiang and Chen's model (2012), and Zhu *et al.*'s model (2015).

A. Qualitative Comparison

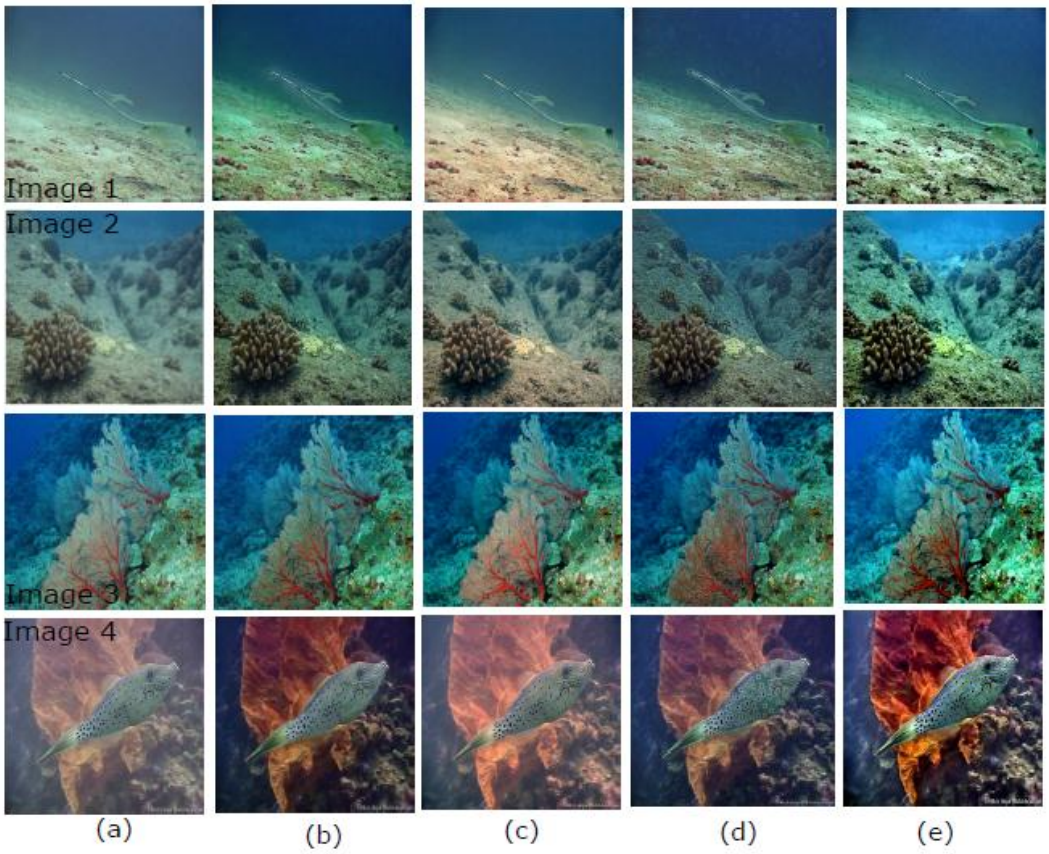

Figure 3. From left to right; Column 1: Input underwater images, Column 2: Results of He et al. (2011),, Column 3: Results of Chiang and Chen (2012), Column 4: Results of Zhu et al. (2015), and Column 5: Results of our proposed method.

Refer Figure 3 for qualitative comparison of the three methods undertaken for comparative study in this paper.

On visual inspection, it is seen that the results offered by He *et al*.'s method suffer from inherent dark regions. Also, block artifacts along the edges are clearly visible in this method as seen in Figure 3(b). In Chiang and Chen's method block artifacts are not observed as seen in Figure 3(c), but this method does not improve the contrast or visibility range. Zhu *et al*.'s method exhibit better visibility, but halos and artifacts are observed as seen in Figure 3(d). Our proposed method on account of image

segmentation produces appealing results. Also, image contrast is enhanced in a better fashion as one can distinguish the objects in the foreground more clearly to those in the background as seen in Figure 3(e). The above-listed improvements prove that the proposed method is able to successfully improve the contrast of the image and exhibit overall natural preservation in color fidelity.

B. Quantitative Analysis

To support our claims of qualitative enhancement and validate our results, we performed quantitative analysis using statistical tools related to image enhancement metrics. This includes visibility metric based on the restoration of edges before and after dehazing, a measure of ability to restore edges, mean ratio of the gradients at visible edges as proposed by [21] and entropy as used in [22].

B.1 Restoration of edges

Enhanced images are expected to have higher visible edges after restoration as compared to the original hazy image [21]. We calculated visible edges before and after restoration and same is shown in Table 2. Our proposed method exhibits a higher number of edges after restoration as compared to other three methods.

Table 2. Visible edges before and after restoration

Image	Original	He *et al*. (2011)	Chiang and Chen (2012)	Zhu *et al*. (2015)	Proposed method
Image 1	34741	56688	44085	58812	63456
Image 2	83220	86966	195735	85315	203727
Image 3	95213	91339	200680	95770	207880
Image 4	25536	80756	37013	80870	101515

B.2 Visibility recovery coefficient *e*

As proposed in [21] and implemented for underwater image qualitative assessment in [12], we calculate parameters *e*, and *r* to compare our results with existing dehazing methods. The value of *e* indicates the measures of ability to restore edges, not visible in the input image but to those observable in the restored image. The value of *e* is calculated by counting the number of edges on the original n_o, and the restored image,n_r as:

$$e = \frac{(n_r - n_o)}{n_o}, \tag{13}$$

We can see in Table 3, our proposed method restores more visibility as compared to other methods.

Table 3. Measure of ability to restore edges, 'e'

Image	He *et al.* (2011)	Chiang and Chen (2012)	Zhu *et al.* (2015)	Proposed Method
Image 1	0.6317	0.2681	0.6928	0.8265
Image 2	-0.4792	0.1700	0.0251	0.2185
Image 3	-0.4600	0.1840	0.0058	0.2272
Image 4	2.1624	0.4494	2.1669	2.9754

B.3 Restoration quality coefficient *r*

Restoration quality coefficient is directly proportional to visibility recovery [21]. Complementary, for every pixel *i* belonging to a visible edge, it computes the ratio of the gradient in the dehazed image and in the original hazy image r_i, and averages it geometrically to obtain the coefficient *r* [12] as:

$$r = \frac{1}{n_r} \sum \log(r_i), \tag{14}$$

The values of *r* in the case of our method is less than He *et al*.'s method for images 2 and 3. It reflects, that He *et al.*'s method has a tendency to retrieve more spurious edges. Table 4 shows restoration quality coefficient using a mean ratio of the gradients at visible edges.

Table 4. Mean ratio of the gradients at visible edges, 'r'

Image	He *et al.* (2011)	Chiang and Chen (2012)	Zhu *et al.* (2015)	Proposed Method
Image 1	1.4057	1.2818	1.6747	2.0663
Image 2	2.2849	1.2390	1.2310	1.8529
Image 3	3.8553	1.1568	1.0808	1.5982
Image 4	1.3433	1.2741	1.6250	2.4015

B.4 Entropy

This image quality metric calculates the information contents in an image that can be used to quantify contrast and edges, which contribute to details in an image. The images with high intensity and hazy veil exhibit lower value of entropy and images with enhanced contrast exhibit retain higher entropy value. The mathematical formulation for image entropy is defined as:

$$H = -\sum_{l=0}^{L-1} P_l log_2 P_l, \tag{15}$$

where L is the number of gray levels, and P_l equals the ratio between the number of pixels whose gray value is $l(0 \leq l \leq L-1)$ and the total pixel number contained in the image [22]. Table 5 demonstrates that our approach is superior to other compared methods.

Table 5. Entropy of images

Image	Original	He *et al.* *(2011)*	Chiang and Chen (2012)	Zhu *et al.* *(2015)*	Proposed method
Image 1	7.1525	7.2267	7.5247	7.1159	7.5296
Image 2	7.1628	7.1980	7.4226	7.1742	7.6928
Image 3	7.4095	7.4006	7.0268	7.0284	7.3309
Image 4	6.7545	6.9332	7.1006	7.0886	7.4052

V. CONCLUSION

A simple yet effective segmentation based approach using pixel based red channel prior for enhancing single underwater images is proposed in this paper. The *k*-means clustering based segmentation introduced here solves the problem of generic homogeneous light. A study conducted on underwater oceanic images revealed that red component plays a vital role in generating a dark channel image on account of its higher attenuation rate, so in this study, we derive the haze depth from the red color channel. A post-processing is included to solve the problem of low contrast by using standard image normalization process. Both quantitative comparison and qualitative comparison exhibits the validity of proposed algorithm by virtue of its restored natural images, color fidelity, and image sharpness. Although this proposed method presented enhanced results, it fails to obtain superior results if the medium light is too dark and under extreme ocean depth, where the red color is totally attenuated or mean intensities are minimal as compared to other channels. A part of the future course of study is to further improve the flexibility and adaptability of proposed algorithm.

REFERENCES

[1] S. Bazeille, L. Jaulin and J. P. Malkasse, "Automatic underwater image pre-processing," in Caracterisation du Milieu Marine (CMM'06), Brest, France, 2006.

[2] Y. V. Schechner, S. G. Narasimhan and S. K. Nayar, "Instant dehazing of images using polarization," in IEEE Proc. of Computer Society Conf. on Computer Vision and Pattern Recognition, Paris, 2001.

[3] S. Shwartz, E. Namer and Y. Y. Schechner, "Blind haze separation," in IEEE

Proc. of Computer Vision and Pattern Recognition, Paris, 2006.

[4] K. He, J. Sun and X. Tang, "Single image haze removal using dark channel prior," IEEE Transactions on Pattern Analysis and Machine Intelligence, vol. 33, no. 12, pp. 2341-2353, 2011.

[5] J. Y. Chiang and Y. C. Chen, "Underwater image enhancement by wavelength compensation and dehazing," IEEE Transactions on Image Processing, vol. 21, no. 4, pp. 1756-1769, 2012.

[6] K. He, J. Sun and X. Tang, "Guided Image filtering," in 11th European Conf. on Computer Vision, Greece, 2010.

[7] H. Lu, Y. Li and S. Serikawa, "Underwater image enhancement using guided trigonometric bilateral filter and fast automatic color correction," in IEEE International Conference on Image Processing, Melbourne, 2013.

[8] S. Serikawa and H. Lu, "Underwater image dehazing using joint trilateral filter," Elsevier Journal of Computers and Electrical Engineering, vol. 40, no. 1, p. 41–50, 2014.

[9] H. Lu, L. Yujie, S. Yang and S. Serikawa, "Adaptive cross image filters for underwater image enhancement," International Journal on Computer, Consumer and Control, vol. 2, no. 1, 2013.

[10] H. Lu, Y. Li, J. Li, X. Li, Y. Kashio and S. Serikawa, "Image contrast enhancement for deep-sea observation systems," in The 3rd International Conference on Industrial Application Engineering, 2015.

[11] N. Carlevaris-Bianco, A. Mohan and R. M. Eustice, "Initial results in underwater single image dehazing," in Proc. IEEE Int. Conf. on Oceans, 2010.

[12] A. Galdran, D. Pardo, A. Picon and A. Alvarez-Gila, "Automatic red-channel underwater image restoration," J. Vis. Commun. Image R., vol. 26, pp. 132-145, 2015.

[13] Q. Zhu, J. Mai and L. Shao, "A fast single image haze removal algorithm using color attenuation prior," IEEE Transactions on Image Processing, vol. 24, no. 12, pp. 3522-3533, 2015.

[14] J. S. Jaffe, "Computer Modelling and the design of optimal underwater imaging systems," IEEE Journal of Oceanic Engineering, vol. 15, no. 2, pp. 101-111, 1990.

[15] S. K. Nayar and S. G. Narasimhan, "Vision in bad weather," in Proc. of the seventh IEEE Conf. on Computer Vision, 1999.

[16] S. G. Narasimhan and S. K. Nayar, "Contrast restoration of weather degraded images," IEEE Transactions on Pattern Analysis and Machine Intelligence, vol. 25, no. 6, pp. 713-724, 2003.

[17] A. S. Abdul, M. Y. Masor and Z. Mohamed, "Colour image segmentation approach for detection of malaria parasiter using various colour models and k-means clustering," WSEAS Transaction on Biology and Biomedecine, vol. 10, 2013.

[18] N. Dhanachandra, K. Manglem and J. Y. Chanu, "Image segmentation using K -means clustering algorithm and subtractive clustering algorithm," in Eleventh International Multi-Conference on Information Processing, Bangalore, India, 2015.

[19] G. Meng, Y. Wang, J. Duan, S. Xiang and C. Pan, "Efficient image dehazing with boundary constraint and contextual regularization," IEEE International Conference on Computer Vision, vol. 25, no. 6, pp. 617-624, 2013.

[20] K. Iqbal, M. Odetayo, A. James, R. A. Salam and A. Z. Talib, "Enhancing the low quality images using unsupervised color correction methods," in IEEE International Conference on Systems Man and Cybernetics, Istanbul, 2010.

[21] N. Hautiere, J. P. Tarel, D. Aubert and E. Dumont, "Blind contrast restoration assessment by gradient ratioing at visible edges," Image Analysis and Stereology, vol. 27, pp. 87-95, 2008.

[22] Y. Yang, D. S. Park, S. Huang and N. Rao, "Medical image fusion via an effective wavelet based approach," EURASIP Journal on Advances in Signal Processing, pp. 1-10, 2010.